Organic & Biomolecular Chemistry

www.rsc.org/obc

Volume 6 | Number 24 | 21 December 2008 | Pages 4469–4672

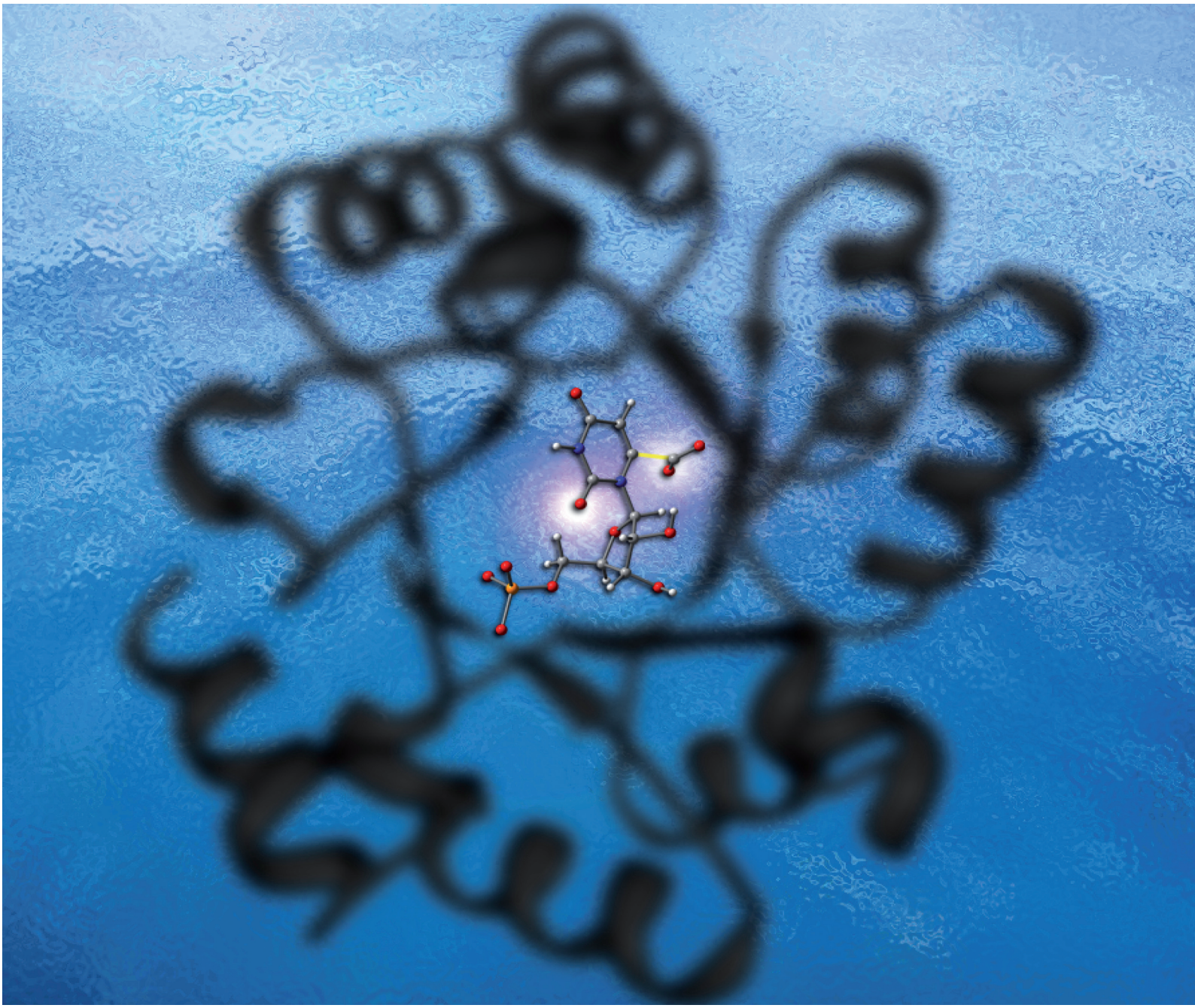

ISSN 1477-0520

RSC Publishing

FULL PAPER

Wickliffe O. Wepukhulu *et al.*

A substantial oxygen isotope effect at O2 in the OMP decarboxylase reaction: Mechanistic implications

Chemical Science

In this issue...

1477-0520(2008)6:24;1-G

A substantial oxygen isotope effect at O2 in the OMP decarboxylase reaction: Mechanistic implications†

Wickliffe O. Wepukhulu,‡[a] Vanessa L. Smiley,§[a] Bhargavi Vemulapalli,¶[a] Jeffrey A. Smiley,*‖[a] Linda M. Phillips[b] and Jeehiun K. Lee*[b]

Received 28th July 2008, Accepted 24th September 2008
First published as an Advance Article on the web 30th October 2008
DOI: 10.1039/b812979g

Orotidine-5′-monophosphate decarboxylase (OMP decarboxylase, ODCase) catalyzes the decarboxylation of orotidine-5′-monophosphate (OMP) to uridine-5′-monophosphate (UMP). Despite extensive enzymological, structural, and computational studies, the mechanism of ODCase remains incompletely characterized. Herein, carbon kinetic isotope effects were measured for both the natural abundance substrate and a substrate mixture synthesized for the purpose of carrying out the remote double label isotope effect procedure, with O2 of the substrate as the remote position. The carbon kinetic isotope effect on enzymatic decarboxylation of this substrate mix was measured to be 1.0199 ± 0.0007, compared to the value of 1.0289 ± 0.0009 for natural abundance OMP, revealing an ^{18}O2 isotope effect of 0.991 ± 0.001. This value equates to an intrinsic isotope effect of approximately 0.983, using a calculated commitment factor derived from previous isotope effect data. The measured ^{18}O2 isotope effect requires a mechanism with one or more enzymatic processes, including binding and/or chemistry, that contribute to this substantial inverse isotope effect. ^{18}O2 kinetic isotope effects were calculated for four proposed mechanisms: decarboxylation preceded by proton transfer to 1) O2; 2) O4; and 3) C5; and 4) decarboxylation without a preceding protonation step. A mechanism involving no pre-decarboxylation step does not appear to have any steps with the necessary substantial inverse ^{18}O2 effect, thus calling into question any mechanism involving simple direct decarboxylation. Protonation at O2, O4, or C5 are all calculated to proceed with inverse ^{18}O2 effects, and could contribute to the experimentally measured value. Recent crystal structures indicate that O2 of the substrate appears to be involved in an intricate bonding arrangement involving the substrate phosphoryl group, an enzyme Gln side chain, and a bound water molecule; this interaction likely contributes to the observed isotope effect.

Introduction

Orotidine-5′-monophosphate decarboxylase (OMP decarboxylase, ODCase; E.C. 4.1.1.23) catalyzes the decarboxylation of orotidine-5′-monophosphate (OMP) to uridine-5′-monophosphate (UMP, eqn 1) and is a key enzyme in the *de novo* pathway of pyrimidine biosynthesis. ODCase has received a degree of attention in the scientific press[1,2] that is unusual for most enzymes. This heightened attention became especially pronounced upon the observation[3] that ODCase displays a catalytic rate enhancement, k_{cat}/k_{uncat}, of $>10^{17}$, a factor then unprecedented, and only surpassed since then by enzymes utilizing cofactors. The cofactor-free ODCase from four microbial sources yielded to crystallographic determination in nearly simultaneous publications in 2000.[4–7] Since those structural studies, the attempts at acquiring mechanistic information using enzymological, computational, and further structural studies have been numerous.[2,8] Nonetheless, the mechanism of ODCase remains incompletely characterized.

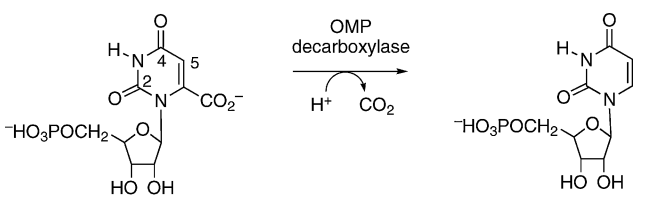

(1)

Several mechanisms for the ODCase-catalyzed reaction have been proposed (Fig. 1). A long-standing mechanistic proposal first advanced by Beak and Siegel[9] arose from the observations of different rates of decarboxylation for model compounds, and involves protonation at O2 of the substrate (Fig. 1A). A second mechanism involving protonation of O4 followed by decarboxylation to yield a stabilized carbene was put forth by Lee

[a]*Department of Chemistry, Youngstown State University, Youngstown, OH 44555, USA. E-mail: j_smiley@acs.org; Tel: +1 (202) 872-6093; Fax: +1 (202) 872-6319*
[b]*Department of Chemistry and Chemical Biology, Rutgers University, Piscataway, NJ 08854, USA. E-mail: jeehiun@rci.rutgers.edu; Tel: +1 (732) 445-6562; Fax: +1 (732) 445-5312*

† Electronic supplementary information (ESI) available: Mass spectrometric data indicating isotope enrichment specifically at the O2 position in uracil, and the double enrichment in [^{18}O,^{13}C-*carboxyl*] OMP. Cartesian coordinates for all calculated species are also available.

‡ Current address: Merck and Co., Inc., West Point, PA, USA.
§ Current address: Panacea Pharmaceuticals, Gaithersburg, MD, USA.
¶ Current address: MedImmune, Gaithersburg, MD, USA.
‖ Permanent address: American Chemical Society, Petroleum Research Fund, 1155 Sixteenth St. NW, Washington, DC 20036, USA.

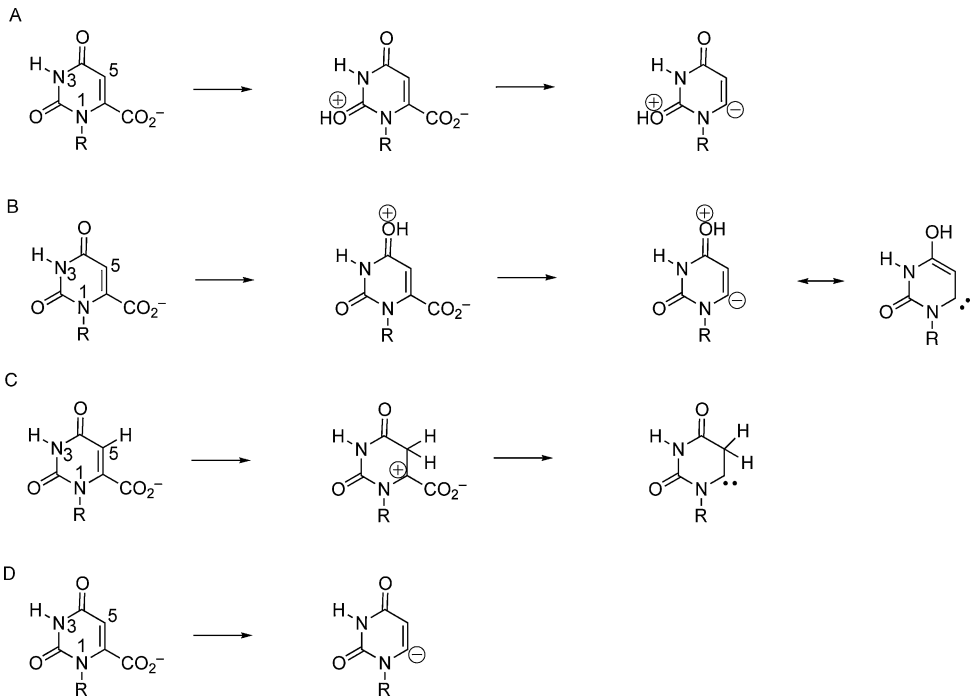

Fig. 1 Four possible mechanisms of ODCase-catalyzed OMP decarboxylation. R = 5-phospho-1-ribosyl (see eqn 1). Protonated intermediates (reactions A–C) are not expected to have isolated positive charges; they are shown as single resonance species to highlight the difference in protonation sites.

and Houk (Fig. 1B).[10] Protonation at C5 has also been proposed (Fig. 1C).[11]

A fourth possibility is direct decarboxylation (Fig. 1D), which does not involve a pre-decarboxylation protonation.[4,6,7,12] This mechanism involves no modifications of the pyrimidine ring, but simply a destabilizing interaction of the substrate carboxylate with the catalytic tetrad Lys44-Asp71-Lys73-Asp76(B) (amino acid numbering from the *E. coli* sequence). The mechanism was predicated on computational studies, even though other computational studies came to different conclusions.[13,14] Variations in direct decarboxylation also exist: some involve generation of a decarboxylated carbanion[6,12] while others do not.[4,7] Recently, a product deuterium isotope effect study[15] and observation of evidence for an anionic intermediate[16] essentially eliminated the possibility of a direct decarboxylation mechanism with no intermediate. The controversial topic of ground state destabilization has been invoked at times to accompany the direct decarboxylation mechanism,[4,6] and subsequently challenged.[17]

Some mechanistic studies indicate the presence of a proton-dependent step prior to decarboxylation in the reaction. The pattern of isotope effects at varying pH[18] suggests a kinetically discernable pH-dependent step for the yeast enzyme, a mechanistic possibility that was supported by the determination of carbon isotope effects in H_2O and D_2O with the ODCase from *Escherichia coli*.[19] Despite this evidence for a pH-dependent step, protonation of the orotate ring to yield a kinetically discernable intermediate prior to decarboxylation was omitted in the formulation of the direct decarboxylation mechanisms, presumably with the assumption that the pH-dependent step was related to protonation elsewhere within the enzyme or substrate.

An examination of nitrogen isotope effects at N1 of OMP[20] has been cited as evidence against mechanisms involving ring protonation, especially protonation at O2 (Fig. 1A). A small, normal N1 isotope effect of 1.0036 was measured for the ODCase reaction using the yeast enzyme; an intrinsic N1 isotope effect of 1.0068 was calculated. The interpretation included an assumption of the equilibrium isotope effect (EIE) for N1 in the O2 protonation mechanism to be comparable to the EIE for N protonation of pyridine, a value that had been previously measured to be 0.979. The use of this substantial inverse EIE in the interpretation appeared to rule out an O2 protonation mechanism, with the reasoning that the O2 protonation step would necessarily contribute to a substantial inverse isotope effect for the measured reaction. A subsequent theoretical analysis,[21] however, indicated a very small N1 EIE of 0.997 upon O2 protonation, much less substantial than that for the EIE for N protonation in pyridine. The bond order of N1 does not change appreciably upon O2 protonation, and thus a small, normal N1 isotope effect would be expected for a mechanism involving OMP protonation at O2. The nitrogen isotope effect data does not appear to distinguish between a mechanism with a small N1 EIE (such as the O2 protonation mechanism) and an N1-independent mechanism.

Very recently, new crystal structures have been presented[22,23] that clarify further the binding and decarboxylation of the substrate OMP. The Inoue and Krungkrai groups[22] have achieved the crystallization of the wild type *Plasmodium falciparum* enzyme in the presence of the substrate. Apparently, the complexation of the active enzyme with substrate did not proceed on to decarboxylation, possibly due to the inability of the crystallized enzyme to undergo a conformational change necessary for catalysis at the low temperatures used. In the *P. falciparum* structure, the substrate binds in an orientation similar to that for the inhibitors seen in previous crystal structures, with the carboxylate in proximity of the catalytic tetrad. The structure of the human ODCase domain

of UMP synthase by the Rudolph group[23] shows the substrate in complex with a highly weakened D312N mutant (corresponding to Asp71 of the *E. coli* sequence); this is a minimal perturbation that essentially maintains the active site volume available for OMP binding. The OMP structure shows a dramatic out-of-plane bending of the labile carboxylate.

However, O2 of the substrate is still seemingly involved in a critical feature of the structure: in the human D312N structure, which may resemble a snapshot of the decarboxylation reaction in progress, the substrate's phosphoryl group closely approaches O2. In fact, one O atom of the phosphoryl group is almost co-linear with the C2-O2 carbonyl group. The two aligned oxygen atoms are bridged, at an angle, by the amide N of Gln430; analogous Gln residues are present in all structures. A bound water molecule is also present in another bridging position between the phosphoryl group and O2 (ref. 23, PDB ID# 2QCL). These features of the structure suggest an intricate network of contacts at O2 that appear important for the reaction. The Gerlt and Richard groups[24] explored this portion of the active site through mutagenesis of the conserved Gln residue and a neighboring Ser residue of the *E. coli* enzyme.

In this paper, we approach the ODCase reaction using oxygen isotope effects in a combined experimental-theoretical study designed to probe the role of O2 of OMP in the ODCase reaction. Experimentally, we utilized ^{18}O enrichment and the double label method described by O'Leary.[25] In this approach, the carbon isotope effect (at the carboxylate carbon) is measured for the enzymatic reaction using the natural abundance substrate. Then, a remote label substrate mixture is synthesized: in the ODCase system, isotopically doubly-enriched OMP contains ^{18}O at O2 and ^{13}C in the carboxylate carbon. Separately, OMP is synthesized with heavy atom depletion at both positions. The natural abundance of ^{18}O is sufficiently low as to be considered isotopically depleted; in this study, the depleted OMP was synthesized with ^{13}C-depleted carbon at the carboxylate position. The isotopically enriched and depleted substrates are then combined so that the ^{13}C (from the enriched OMP) is near natural abundance, requiring a ratio of approximately 1:90 of the doubly-enriched to doubly-depleted OMP. The carbon isotope effect for the enzymatic reaction using this mixture is then measured; the ratio of the two carbon isotope effects is equal to the isotope effect at O2 for the enzymatic reaction. We measured carbon isotope effects for natural abundance OMP and an OMP remote label mixture in order to probe the possible reaction mechanisms for the ODCase reaction. Isotope effects were calculated for several possible mechanistic steps and compared to the experimental result in order to determine which mechanisms could be supported.

Results and discussion

Measurement of the isotope effects

Uracil synthesized by the method described, with $H_2{}^{18}O$ hydrolyzing the 2-ethylthio group, showed a molecular weight of 114 (anion = 113), with very little MW = 112 and MW = 116 (see Supplementary Materials), indicating nearly exclusive incorporation of ^{18}O into only the 2-position. This ^{18}O-enriched compound was stable to 0.5 M NaOH, with no observable conversion of MW = 114 to MW = 112 (see Supplementary Materials). This stability was necessary to preserve isotopic enrichment throughout the synthesis of OMP. The complete synthesis of [$^{18}O2$, ^{13}C-*carboxyl*] OMP resulted in high isotopic enrichment at both positions, indicated from the predominant anion MW = 370 *versus* anion MW = 367 for natural abundance OMP (see Supplementary Materials).

Table 1 Carbon kinetic isotope effects using OMP synthesized for the remote double label method[a]

$\delta\,^{13}C$	f	^{13}k
Natural abundance OMP		
−72.70	0.389	1.0282
−52.46	1.0	
−72.65	0.459	1.0300
−52.46	1.0	
−71.88	0.326	1.0278
−50.80	1.0	
−69.70	0.48	1.0295
−50.25	1.0	
$^{13}k = 1.0289 \pm 0.0009$		
Remote label OMP mixture[b]		
−34.12	0.30	1.0211
−17.15	1.0	
−25.64	0.595	1.0198
−13.74	1.0	
−52.85	0.44	1.0193
−39.33	1.0	
−53.61	0.37	1.0192
−39.33	1.0	
$^{13}k = 1.0199 \pm 0.0007$		
^{18}O effect = 0.991 ± 0.001		

[a] f: fraction of reaction. ^{13}k: carbon kinetic isotope effect measurement, calculated from the two measured $\delta\,^{13}C$ values and the corresponding f values for the partial reaction. [b] "Remote Label OMP Mixture" refers to the substrate mixture described in the text: a mixture of [$^{18}O2$, ^{13}C-*carboxyl*] OMP, and OMP depleted in both positions. The ratio of the two isotope effects is equal to the ^{18}O effect on the carbon kinetic isotope effect.

A sample of 10 μmol of isotopically depleted OMP was decarboxylated with ODCase, in order to assess the level of ^{13}C depletion. The CO_2 collected showed a delta value of −370 (cf., delta value of CO_2 from natural abundance OMP ≈ −50), indicating extensive ^{13}C depletion.

The carbon kinetic isotope effect for *E. coli* ODCase measured in this study, for the natural abundance substrate, was 1.0289 ± 0.0009, at pH 7.0, 25 °C (Table 1). This can be compared with the previously reported value[19] of 1.043 ± 0.003, at pH 7.5. *E. coli* ODCase thus displays a sharp increase in the kinetic isotope effect of decarboxylation as the pH is raised above neutral, a trait that was also described for the yeast ODCase.[18]

The carbon kinetic isotope effect for ODCase with the remote label substrate mixture, to assess the isotope effect at O2, was 1.0199 ± 0.0007 (Table 1). This isotope effect was essentially independent of composition of the remote label substrate mix; different mixes gave the same result. The ratio of the two kinetic isotope effects, 0.991 ± 0.001, indicates the isotope effect at O2 for the overall reaction.

Since the enrichment and depletion of isotopes in the remote label OMP mixture are not complete, a small correction to the measured value can be made using the equations described by Cleland.[26] Using 97% enrichment for ^{18}O (from the ^{18}O water used in the synthesis), 99% enrichment for ^{13}C (from the $^{13}CN^-$ used) and 0.2% natural abundance ^{18}O in the depleted OMP, the measured effect of 0.991 corrects to 0.990. Using 98.5% enrichment for ^{18}O

and 99.5% enrichment for ^{13}C in the calculation also results in the correction to 0.990.

Measurement of the ODCase isotope effect under neutral conditions does not allow observation of any intrinsic isotope effect, due to the presence of a substantial commitment factor.[18,20] The largest ^{13}C carboxylate KIE measured for ODCase, 1.0506, is likely very close to the intrinsic ^{13}C carboxylate IE. Using this value, and the ^{13}C carboxylate KIE of 1.0289 under conditions used herein, a commitment factor of 0.75 can be calculated. Applying this commitment factor to the $^{18}O2$ effect yields an intrinsic $^{18}O2$ isotope effect of 0.983. The error in this value is difficult to predict, due to the uncertainty of the intrinsic ^{13}C carboxylate IE and uncertainty about whether or not the commitment factor for the ^{13}C-carboxyl position is identical to the commitment factor for $^{18}O2$, so this value will be considered approximate in the ensuing discussion.

Interpretation of the O2 isotope effect

The mechanism for ODCase decarboxylation of OMP must include binding and chemical steps which, taken together, account for the substantial $^{18}O2$ isotope effect of 0.983. In a multi-step enzymatic reaction, small isotope effects may arise at almost any step. The overall IE will be the product of IEs on all steps up to and including the first irreversible step in the reaction; for the ODCase reaction under our conditions, the decarboxylation step can be assumed to be irreversible. Previous isotope effects measured in H_2O and D_2O evidenced the presence of a pH-dependent pre-decarboxylation step.[19] In consideration of a minimal kinetic mechanism, where ES† is an activated intermediate (eqn 2):

$$E + S \underset{}{\overset{A}{\rightleftharpoons}} ES \overset{B}{\rightleftharpoons} ES^{\dagger} \xrightarrow{C} E + P \qquad (2)$$

all possible ODCase mechanisms must involve substrate binding (A) and decarboxylation (C).

The various protonation mechanisms propose formation of kinetically discernable protonated intermediates (Fig. 1) that would account for Step B in eqn 2. Step B in the direct decarboxylation mechanism must be a chemical or conformation step that does not involve chemistry at the orotate ring.

An isotope effect on Step A can arise from a number of factors not involving direct contact of the enzyme with the isotopic position, as recently reviewed by Schramm.[27] In the case of ODCase, at least two factors are possibly involved: desolvation of the substrate, and restricted molecular motion upon binding. Desolvation of O2 of OMP would likely contribute a normal (>1) component to the ^{18}O effect for the overall reaction. The desolvation of formate in the formate dehydrogenase reaction was predicted to have a small, normal contribution to the overall ^{18}O IE.[28] Transfer of water into the vapor phase is accompanied by an ^{18}O IE of 1.009.[29] O2 of OMP would seem to be less highly solvated than formate (charged) or water molecules, so the desolvation contribution to the isotope effect in the case of the ODCase reaction would likely be minimal.

Restricted torsional motions of a substrate upon binding to an enzyme active site are also known to contribute to an IE for an enzyme reaction. A thoroughly discussed example of ^{18}O effects is given for two enzyme reactions that utilize phosphoenolpyruvate (PEP), examining the effects at the C–O–P bridging oxygen.[30] The ^{18}O effect at this position upon binding and restriction of torsional motion is an inverse effect in the range of 0.994. It seems reasonable to assume that torsional motions at O2 of OMP will not be as significantly affected as is the case for the bridging oxygen in PEP: both the C–O and O–P bonds are freely rotatable in PEP, while O2 of OMP does not have the same role in conformational flexibility as the bridging oxygen of PEP.

These two effects possibly contributing to Step A are therefore small and opposite to each other, and taken together likely contribute no more than 0.003 in either direction to the overall ODCase ^{18}O IE.

$^{18}O2$ isotope effects for decarboxylation steps were calculated for the three proposed protonated intermediates as well as for unprotonated OMP. In every case, the ^{18}O IE was calculated to be small and normal; a range of 1.003 to 1.006 was found (Fig. 2). The direction of this isotope effect is predictable, since decarboxylation results in increased electron density on the ring and thus a longer C–O2 bond in the transition state. Such a reaction would be slightly faster for ^{16}O than for ^{18}O, giving rise to a normal isotope effect.

For the direct decarboxylation mechanism to be congruent with the observed data, it is apparent that a large contribution to the $^{18}O2$ isotope effect of 0.983 present in the ODCase reaction would have to come from Step A. The assumption that Step B does not involve chemistry on the orotate ring would require that that step is isotopically insensitive, or essentially insensitive, at O2. Since the decarboxylation step (C) is expected to contribute a normal isotope effect of 1.004–1.005, step A must contribute a factor in the range of 0.980–0.985 to the observed effect.

In an attempt to gain information on the isotope effect at O2 upon binding, we calculated the equilibrium IE associated with simple hydrogen bond formation between O2 of 1-methylorotate and the NH of formamide, in a geometry similar to that seen in the ODCase crystal structures (Fig. 3). The effect of hydrogen bonding was explored by calculating the isotope effect associated with the complexation of 1-methyl orotate with acetamide (which mimics glutamine; details in Computational methods section). The isotope effect associated with acetamide forming two hydrogen bonds as shown in Fig. 3 is 0.9998. Therefore, this routine hydrogen bonding and a pre-decarboxylation step not involving bond-making on the orotate ring in the direct decarboxylation mechanism cannot account for the measured substantial $^{18}O2$ effect if the effects for the proposed individual steps are consistent with our modeled values.

In a further attempt to interpret the $^{18}O2$ isotope effect, we calculated equilibrium IEs associated with the individual protonation steps for the mechanisms in Fig. 1, using N1-methyl orotate as the substrate.[21] The calculated EIEs for the equilibrium in the gas phase are shown in Fig. 2, above the equilibrium arrows. For the O2 protonation mechanism (Fig. 2A), the initial proton transfer is associated with an inverse $^{18}O2$ EIE of 0.993.

Intriguingly, the $^{18}O2$ EIE for the O4 protonation (Fig. 2B) is similar, 0.994. This is somewhat surprising since one might expect a much more substantial inverse IE for protonation at O2 than at O4, since the ^{18}O substitution is at O2. However, these isotope effects arise not only from new bond formation at enriched positions (as for the O2 protonation mechanism) but also from changes in geometry, and O4 protonation incurs a shortening of the C–O2 bond, leading to the inverse IE. Protonation of O2 results in a new bond at the labeled position, which would contribute to an inverse IE, but the C–O2 bond becomes longer, contributing a normal

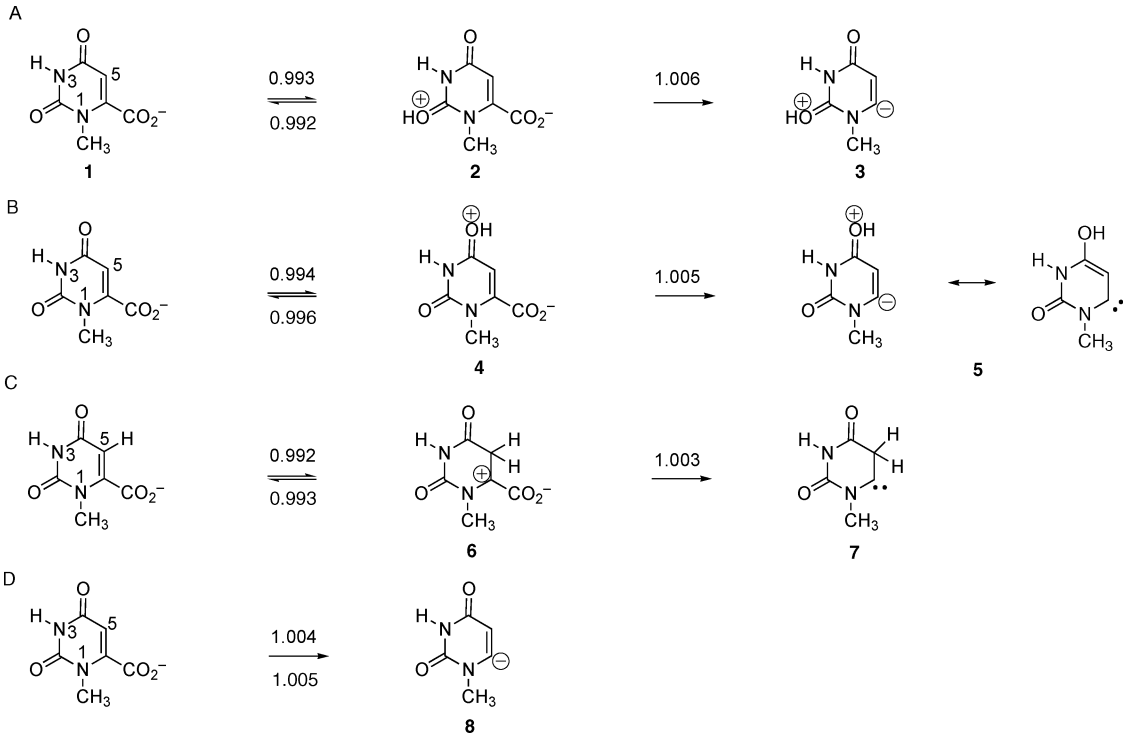

Fig. 2 Calculated isotope effects for possible ODCase mechanisms. Gas phase values for the protonation equilibria are above the equilibrium arrows; values in a water dielectric are below the arrows.

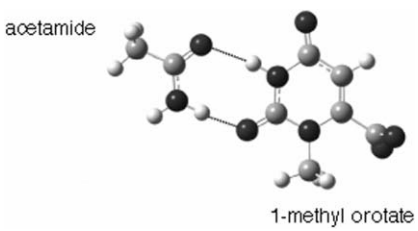

Fig. 3 Calculated optimized complex of acetamide and 1-methyl orotate, at B3LYP/6-31 + G*.

component to the IE and resulting in a protonation EIE value that is similar to that of protonation at O4. The C5 protonation mechanism (Fig. 2C) has a calculated protonation EIE of 0.992.

In an attempt to model a more enzyme-like environment, we also calculated the EIE for the protonation step in a water dielectric. We find that the values do not drastically change when solvent is taken into account (Fig. 2, water values below equilibrium arrows). The O2 protonation is slightly more inverse in water than in the gas phase, but by very little (0.993 gas phase, 0.992 in water). The O4 protonation shows the greatest change, from an EIE of 0.994 in the gas phase to 0.996 in water. The C5 protonation mechanism remains essentially constant (0.992 in the gas phase, 0.993 in water). The direct decarboxylation mechanism is also barely affected by solvation and stays firmly normal (IE of 1.004 in gas phase, 1.005 in water). In essence, the general trends remain unchanged: the protonation steps are characterized by an inverse ^{18}O2 IE, and decarboxylation has a normal ^{18}O2 IE.

These calculated EIE values for protonation are somewhat small, and another feature of the reaction is likely necessary to fully account for the ^{18}O2 effect of approximately 0.983. An interesting literature precedent for ^{18}O isotope effects on binding is found in the study of lactate dehydrogenase (LADH) and its interaction with [1-^{18}O] oxamate, a substrate analog.[31] The ^{18}O effect on binding was measured to be 0.984 ± 0.003; this effect is attributable to an intricate interaction of the labeled carboxylate group of oxamate with two guanidinium groups from arginine side chains and a threonine hydroxyl group. In the LADH-oxamate structure,[32] either oxygen in the carboxylate group will be involved in two hydrogen bonding or charge interactions with functional groups at the active site, regardless of the orientation of the labeled oxygen in the carboxylate. An isotope effect of this magnitude in the ODCase-OMP interaction would almost completely account for the approximate observed value of 0.983, with small effects from the other steps factored in.

The orientation of O2 in the new ODCase-OMP structures[22,23] indicates a significant interaction of O2 with the substrate phosphoryl group, an enzyme Gln side chain, and a bound water molecule. This interaction, which may involve proton transfer or hydrogen bonding, appears to offer an explanation for the observed isotope effect data. Considering the enormous (11 orders of magnitude) decrease in ODCase activity toward orotidine nucleosides lacking phosphoryl groups[33] and the rescue of activity using phosphite,[34] and the very large (at least 7 orders of magnitude) decrease in ODCase activity toward 2-thioOMP,[35] this proposed feature of the enzyme reaction, which still remains incompletely characterized, seems critical to enzyme activity.

Although the collection of functional groups in the proximity of O2 in the ODCase-OMP structure appears more intricate than that at O4 or C5, there does not appear to be any firm experimental data yet presented that excludes the proposed mechanisms of protonation at these sites. It should be noted that most depictions

of ODCase active sites omit the presence of enzyme-bound water molecules, which have been proposed to be proton transfer conduits.[36]

Experimental

Production of *E. coli* ODCase

The ODCase gene from *E. coli*[37] was amplified using PCR, for insertion into the *NdeI* and *HindIII* restriction sites of plasmid pCAL-n (Stratagene). Oligonucleotide primers for PCR were obtained from Integrated DNA Technologies, Inc., and have the following sequences (restriction sites underlined):

5′ primer: 5′-GGGAAAGGCATATGACGTTAACTGCTTC-ATCTTC-3′

3′ primer: 5′-GGAAAGGAAAGCTTTCATGCACTCCGC-TGTAAAGAGG-3′

Thermostable DNA polymerase from New England Biolabs was used in a standard PCR mixture with the above primers and a preparation of *E. coli* genomic DNA.[38] The resulting 0.8 kbp PCR product was purified, digested with NdeI and HindIII (NEB), purified again and ligated to pCAL-n digested with the same restriction enzymes, using T4 DNA ligase (NEB). The ligation mix was used for transformation of *E. coli* XLI-Blue to give ampicillin resistance, and potentially correct plasmid constructions from transformants were screened by gel electrophoresis of plasmid preparations. Plasmids appearing to contain the ODCase gene were introduced into *E. coli* BL21 (DE3)-Gold cells (Stratagene). Protein lysates from cultures carrying this plasmid and induced with IPTG (50 μM; incubation continued at 37 °C for 6 hrs after IPTG addition to mid-log culture in LB media) showed vastly increased levels of ODCase activity *versus* uninduced cells,[39] based on ODCase spectrophotometric assays.[40]

ODCase was purified using Affi-Gel Blue (BioRad) chromatography, using a method similar to that previously described,[41] except that ODCase could be eluted from the column using 1 mM UMP instead of the stronger inhibitor 6-azaUMP used previously. Dialysis of the pooled, concentrated fractions resulted in a decrease of UMP concentration to a very low level,[39] as analyzed by HPLC (see HPLC section below). ODCase prepared by this method appeared as a single predominant band on gel electrophoresis, with specific activity of 55 nmol min^{-1} μg^{-1}.[39]

Standard HPLC conditions for analysis of nucleotides

Using a Waters 1525 dual pump HPLC (Breeze System software), a gradient of water as solvent A and 0.8 M NH_4HCO_3 as solvent B was run at a flow rate of 2 mL min^{-1} with the following setup: 0 min, 100% A, 0% B; 20 min, 0% A, 100% B. The column was a PRP-X100 anion exchange column (250 mm × 4.6 mm, Hamilton). Elution was analyzed spectrophotometrically at 280 nm, except in the case of the monitoring of the fraction of conversion of OMP to UMP (see below), in which case the wavelength was 264 nm. Injections of standard nucleotide solutions (100 nmol nucleotide) were performed to yield peaks for general retention times of each nucleotide: UMP (6.4 min), 5-Br-UMP (9.3 min), 6-CN-UMP (11.0 min), OMP (7.2 min).

Standard ion exchange chromatography conditions for purification of nucleotides

Nucleotide solutions were applied to a column (2.5 cm diameter and lengths from 20 to 28 cm) filled with Dowex 1 × 8–200 anion exchange resin (Sigma/Aldrich) washed with 0.8 M NH_4HCO_3 and rinsed with dH_2O. A gradient from 0 to 0.8 M NH_4HCO_3 (0.5 L of each) was used for elution, with additional 0.8 M NH_4HCO_3 used for continued elution as necessary. Fractions (8 mL) containing nucleotide were identified by UV absorbance and subsequently analyzed by HPLC (as described above). Fractions containing the desired nucleotide were pooled and desalted with Dowex HCR-W2 cation exchange resin (Sigma/Aldrich), which was washed prior to desalting with 1 M HCl and then rinsed with dH_2O until the rinsings were neutral. Enough resin was added to the nucleotide solution so that the pH was lowered to less than 4. Resin was removed by filtration and solutions were evaporated to a desired concentration, or dryness. Final concentrations were determined spectrophotometrically at absorbances appropriate to the specific nucleotide.[42]

Synthesis of [^{18}O2, ^{13}C-*carboxyl*] OMP

2-Thiouracil was converted to 2-ethylthiouracil (Fig. 4, Step 1) *via* a reaction of 1.0 g of 2-thiouracil (Aldrich) with 1.2 g iodoethane in 15 mL DMF, with heating at 60 °C under reflux. The product was purified by silica gel chromatography using a solvent of 2:3 hexane/ethyl acetate.

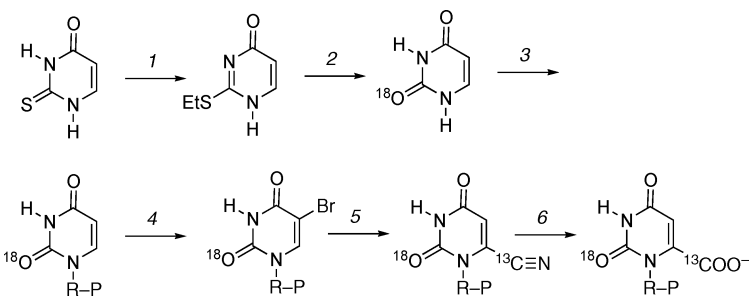

Fig. 4 Synthetic scheme for [^{18}O2, ^{13}C-*carboxyl*] OMP. Details are described in the text. Step 1: Alkylation of 2-thiouracil with iodoethane. Step 2: Hydrolysis of 2-ethylthiouracil with acidified $H_2{}^{18}O$. Step 3: Conversion of [^{18}O2] uracil to [^{18}O2] UMP with UPRTase and PRPP. Step 4: Conversion of [^{18}O2] UMP to [^{18}O2] 5-bromo-UMP using Br_2. Step 5: Conversion of [^{18}O2] 5-bromo-UMP to [^{18}O2, ^{13}C-*cyano*] 6-cyano-UMP using NaCN or KCN. Step 6: Hydrolysis of [^{18}O2, ^{13}C-*cyano*] 6-cyano-UMP to [^{18}O2, ^{13}C-*carboxyl*] OMP using aqueous NaOH. Steps 4–6 were used for the synthesis of natural abundance and isotopically-depleted OMP, using natural abundance or isotopically-depleted reagents. R–P = 5-phospho-1-ribosyl.

2-Ethylthiouracil was converted to [^{18}O2] uracil (Fig. 4, Step 2) by acid-catalyzed hydrolysis in acidified $H_2{}^{18}O$. HCl gas was bubbled through $H_2{}^{18}O$ (> 97% ^{18}O, Cambridge Isotope Laboratories) until the resulting solution was thoroughly acidic. 200 mg of 2-ethylthiouracil was added to 1 mL of acidified $H_2{}^{18}O$; the reaction vial was sealed, vented with a hypodermic needle, and heated at 70 °C. Evolution of gas (thioethane) was observed, and the heating continued until gas evolution ceased. Samples of the reaction mix were analyzed by TLC (1:19 methanol/ethyl acetate solvent) with 2-ethylthiouracil and uracil standards; heating was resumed until no more 2-ethylthiouracil could be observed in the reaction mix. The resulting uracil was analyzed using a Bruker Esquire mass spectrometer, under electrospray ionization conditions for anion detection.

To determine whether the pyrimidine ^{18}O2 was stable to base hydrolysis conditions, in anticipation of the conversion of [^{18}O2, 6-^{13}C-*cyano*] 6-CN-UMP to OMP, approximately 1 mg of [^{18}O2]-uracil was placed in solutions containing a final concentration of 0.5 M NaOH and held at room temperature for up to 8 days. Samples were periodically taken and analyzed by LC-MS to observe whether an exchange of natural abundance oxygen from water could be detected, as indicated by conversion of the molecular weight of 114 (for [^{18}O2]-uracil) to 112 (for natural abundance).

[^{18}O2] uracil was converted to [^{18}O2] UMP (Fig. 4, Step 3) using recombinant UPRTase and the co-substrate PRPP (Fluka). The UPRTase gene from genomic *E. coli* DNA[43] was amplified by PCR in a manner similar to the cloning of the *E. coli* ODCase gene, with the following primers (IDT, Inc.) used:

5′ primer: 5′-AGGTACATATGAAGATCGTGGAAGTCA-AA-3′

3′ primer: 5′-AGGTAAAGCTTTTATTTCGTACCAAAGAT-TTT-3′

Plasmids appearing to contain the UPRTase gene were introduced into BL21 (DE3)-Gold cells. Protein lysates from cultures induced with IPTG (as above for ODCase production) showed vastly increased levels of a protein of 22.5 kD, as analyzed by polyacrylamide gel electrophoresis, *versus* uninduced cells.[44] Protein lysates were used for conversion of uracil to UMP without purification.

Initial UPRTase reactions (1 mL volume) were performed using 1 mg unenriched uracil, 25 mM Tris-HCl, pH 8.6, 5 mM $MgCl_2$, 2 mg BSA, as previously described.[45] Each reaction was started by addition of 5.5 mg PRPP and protein (typically 5 μL of lysate) carried out at 37 °C with gentle shaking. Reactions for [^{18}O2]-UMP synthesis were scaled up proportionally to a total volume of 6 mL. The appearance of UMP was monitored by HPLC as described above. Once the conversion to [^{18}O2]-UMP was near completion (>95% converted), the samples were frozen until purification could be carried out. Purification was performed using anion exchange chromatography as described above. After purification, the [^{18}O2]-UMP was analyzed by LC-MS, as above, to ensure retention of ^{18}O enrichment.

Synthesis of [^{18}O2, ^{13}C-*carboxyl*] OMP from [^{18}O2]-UMP (Fig. 4, Steps 4–6) was carried out as described below for natural abundance OMP, except that Na^{13}CN or K^{13}CN (99% ^{13}C, Cambridge Isotope Laboratories) was used in place of unenriched NaCN. No difference could be observed in the rates or products of reaction with Na^{13}CN *versus* K^{13}CN. After synthesis, the [^{18}O2, ^{13}C-*carboxyl*]-OMP was analyzed by LC-MS, as above, to ensure retention of ^{18}O and ^{13}C enrichment.

Synthesis of natural abundance OMP

Conversion of UMP (Sigma-Aldrich) to OMP by the method of Ueda *et al.*[42] was used with the following modifications: 1) (Fig. 4, Step 4) 5-Br-UMP was purified from its reaction solution by evaporation to dryness and application of the redissolved (aqueous) solution to the standard ion exchange chromatography conditions (above). 2) (Fig. 4, Step 5) 6-CN-UMP formation was monitored using HPLC (above conditions) and the desired product was again purified using the standard ion exchange chromatography conditions (above). 3) (Fig. 4, Step 6) Conversion of 6-CN-UMP to OMP was found to proceed to completion, with formation of essentially no detectable by-products, using 0.5 M NaOH at room temperature for 4 days. The OMP solution was neutralized with Dowex HCR-W2 cation exchange resin, as above, and used without further purification.

Synthesis of OMP (^{13}C-depleted in the carboxylate)

This synthesis was carried out as described above for synthesis of natural abundance and enriched OMP, except that ^{13}C-depleted KCN (> 99.9% ^{12}C, Icon Isotopes, Summit, NJ) was substituted for natural abundance NaCN.

Measurement of carbon isotope effects

General procedures were taken from O'Leary.[25] CO_2 samples were analyzed for carbon isotope content using an Isoprime Dual Inlet isotope ratio mass spectrometer (GV Instruments, Inc.). Reference gas was natural abundance CO_2 (Praxair), which was analyzed to have a ^{13}C delta value of 0.21 *versus* Vienna PDB at the Cornell University Stable Isotope Laboratory (Art Kasson, Lab Manager).

Reactions for CO_2 collection and distillation were performed in flasks designed to avoid contamination by atmospheric CO_2. Reaction mixtures contained 5 mM OMP and 50 mM MOPS, pH 7.0. Reaction mixtures were sparged with Drierite-scrubbed N_2 prior to addition of enzyme. Reactions were initiated by the addition of ODCase and terminated by the addition of H_2SO_4 to pH < 2. Partial reactions (30 μmol OMP) were carried out at 25 °C in a water bath, with enough enzyme added to convert about 30% of the substrate to product within a few minutes. For every partial reaction, a complete reaction (typically 5-fold amount of ODCase, 5-fold reaction time *versus* partial reactions) containing 10 μmol OMP was performed, and checked for completion by HPLC. Collection of CO_2 was carried out using a specially designed glass cryodistillation system under vacuum, similar to previous work.[18]

The composition of the remote label OMP mixture (double-enriched plus depleted) was adjusted so that CO_2 generated from a complete reaction (10 μmoles) had a delta value approximately equal to that of the natural abundance OMP. OMP mixtures that yielded CO_2 with a highly positive delta value, for example, were supplemented with more depleted OMP.

Fractions of reactions were determined following CO_2 collection by HPLC analysis (above) of OMP and UMP, using a UV detection wavelength of 264 nm. At this wavelength, OMP and UMP have equal extinction coefficients, since this is the isosbestic

point in the spectrophotometric assay. Peaks emerging from the HPLC were integrated by the Breeze Software system to determine the fraction of reaction. Using the fraction of reaction, and the delta values for partial and complete reactions, isotope effects were calculated for the ODCase reaction with natural abundance OMP, and the OMP remote label mixture, using the calculations previously described.[18]

Computational methods

Ground-state and transition structures were fully optimized using B3LYP/6-31 + G* calculations as implemented in Gaussian98 and Gaussian03.[46,47] B3LYP methods have been previously shown to provide reliable energetics for decarboxylation reactions.[10,21,48–51] A vibrational frequency analysis was performed on all stationary points. To allow for solvation effects, structures **1**, **2**, **4**, **6** and **8** were also optimized using the Onsager solvent model in water.[52] Equilibrium and kinetic isotope effects were calculated both in the gas phase and in water (using the Onsager solvent-model structures) at 298 K using the formulation of Bigeleisen and Meyer.[53–56] A vibration scaling factor of 0.96 was used for both the gas phase and solvent calculations.[57] The Onsager method has been shown to give reliable geometries and isotope effects in recent studies of the enzyme *N*-methyltryptophan oxidase.[58]

The effect of a hydrogen bond on O2 of OMP was explored *via* a model based on the crystal structure of *Bacillus subtilis* OMP decarboxylase with bound UMP.[4] Gln194 and UMP were extracted from an arbitrarily selected subunit of the crystal structure (1DBT). This structure was modified by replacing the sugar moiety with a methyl group, and by reducing Gln194 to acetamide. A carboxylate was added to UMP in an orientation consistent with the optimized geometry of 1-methylorotate. Coordinates of the heavy atoms originating from the crystal structure were not altered. This hydrogen-bonded complex of 1-methylorotate and acetamide was fully optimized in the gas phase at B3LYP/6-31 + G* and equilibrium isotope effect calculations were conducted.

Conclusions

We have measured an ^{18}O2 isotope effect for the ODCase decarboxylation reaction of 0.991 ± 0.001, which leads to the calculation of an intrinsic ^{18}O effect of approximately 0.983. This substantial ^{18}O2 effect requires a mechanism that includes one or more steps associated with binding and pre-decarboxylation chemistry with significantly inverse contributions to this overall effect. The direct decarboxylation mechanism proposes no bond forming events on the orotate ring prior to the decarboxylation step, and the calculated ^{18}O2 IEs for such a mechanism do not appear able to account for the experimental value. New structures of the ODCase-OMP complex show an intricate network of contacts between O2, the substrate phosphoryl group, an enzyme Gln side chain, and a bound water molecule; this feature of the active site appears critical for decarboxylation and may account for the observed isotope effect data.

Acknowledgements

Assistance from Dr. Roland Riesen, Youngstown State University, in obtaining mass spectrometric analyses of isotopic incorporation into uracil and other compounds is gratefully acknowledged. We thank Art Kasson, Cornell University, for analysis of standard CO_2. Special thanks to Melisa Kundracik (current address: Department of Biochemistry, Brandeis University), who composed a lab manual on the use of the isotope ratio mass spectrometer and CO_2 distillation line during a PRF-supported summer research project. Special thanks also to Dr. Howard Mettee, Department of Chemistry, Youngstown State University, for keeping the CO_2 distillation line operating following occasional mishaps.

This work was supported by the American Chemical Society Petroleum Research Fund, Grant #39730-B4, an instrumentation grant from the Ohio Board of Regents Hayes Investment Fund to the Ohio Mass Spectrometry Consortium, and partially by grant GM63504–01 from the National Institutes of Health AREA Program (WOW, VLS, BV, JAS).

JAS has been a program officer at ACS PRF since July 2006, and had no affiliation with PRF at the time Grant #39730-B4 was awarded (May 2003).

JKL and LMP gratefully acknowledge the support of NSF, the Alfred P. Sloan Foundation, the Rutgers Busch Grant Program and the National Center for Supercomputer Applications. We also thank Professor Daniel Singleton for helpful discussions and use of his version of the Quiver program.

References

1 A. M. Rouhi, *Chemical & Engineering News*, 2000, **78**, 42–46.
2 *Orotidine monophosphate decarboxylase : a mechanistic dialogue*, Springer, Berlin, 2004.
3 A. Radzicka and R. Wolfenden, *Science*, 1995, **267**, 90–93.
4 T. C. Appleby, C. Kinsland, T. P. Begley and S. E. Ealick, *Proc. Natl. Acad. Sci. USA*, 2000, **97**, 2005–2010.
5 B. G. Miller, A. M. Hassell, R. Wolfenden, M. V. Milburn and S. A. Short, *Proc. Natl. Acad. Sci. USA*, 2000, **97**, 2011–2016.
6 N. Wu, Y. Mo, J. Gao and E. F. Pai, *Proc. Natl. Acad. Sci. USA*, 2000, **97**, 2017–2022.
7 P. Harris, J. C. Navarro Poulsen, K. F. Jensen and S. Larsen, *Biochemistry*, 2000, **39**, 4217–4224.
8 B. G. Miller and R. Wolfenden, *Annu. Rev. Biochem.*, 2002, **71**, 847–885.
9 P. Beak and B. Siegel, *J. Am. Chem. Soc.*, 1976, **98**, 3601–3606.
10 J. K. Lee and K. N. Houk, *Science*, 1997, **276**, 942–945.
11 T.-S. Lee, L. T. Chong, J. D. Chodera and P. A. Kollman, *J. Am. Chem. Soc.*, 2001, **123**, 12837–12848.
12 S. Hur and T. C. Bruice, *Proc. Natl. Acad. Sci. USA*, 2002, **97**, 9668–9673.
13 M. Lundberg, M. R. A. Blomberg and P. E. M. Siegbahn, *J. Mol. Model.*, 2002, **8**, 119–130.
14 C. L. Stanton, I.-F. W. Kuo, C. J. Mundy, T. Laino and K. N. Houk, *J. Phys. Chem. B*, 2007, **111**, 12573–12581.
15 K. Toth, T. L. Amyes, B. M. Wood, K. Chan, J. A. Gerlt and J. P. Richard, *J. Am. Chem. Soc.*, 2007, **129**, 12946–12947.
16 T. L. Amyes, B. M. Wood, K. Chan, J. A. Gerlt and J. P. Richard, *J. Am. Chem. Soc.*, 2008, **130**, 1574–1575.
17 A. Warshel, M. Strajbl, J. Villa and J. Florian, *Biochemistry*, 2000, **39**, 14728–14738.
18 J. A. Smiley, P. Paneth, M. H. O'Leary, J. B. Bell and M. E. Jones, *Biochemistry*, 1991, **30**, 6216–6223.
19 J. I. Ehrlich, C.-C. Hwang, P. F. Cook and J. S. Blanchard, *J. Am. Chem. Soc.*, 1999, **121**, 6966–6967.
20 M. A. Rishavy and W. W. Cleland, *Biochemistry*, 2000, **39**, 4569–4574.
21 L. M. Phillips and J. K. Lee, *J. Am. Chem. Soc.*, 2001, **123**, 12067–12073.
22 K. Tokuoka, Y. Kushakari, S. R. Krungkrai, H. Matsumura, Y. Kai, J. Krungkrai, T. Horii and T. Inoue, *J. Biochem.*, 2008, **143**, 69–78.
23 J. G. Wittmann, D. Heinrich, K. Gasow, A. Frey, U. Diederichsen and M. G. Rudolph, *Structure*, 2008, **16**, 82–92.
24 S. A. Barnett, T. L. Amyes, B. M. Wood, J. A. Gerlt and J. P. Richard, *Biochemistry*, 2008, **47**, 7785–7787.

25 M. H. O'Leary, in *Methods in Enzymol.*, Academic Press, New York, 1980, vol. 64, pp. 83-104.
26 W. W. Cleland, *Enzyme mechanisms from isotope effects*, CRC Press, Boca Raton, FL, 2006.
27 V. L. Schramm, *Curr. Opin. Chem. Biol.*, 2007, **11**, 529–536.
28 J. D. Hermes, S. W. Morrical, M. H. O'Leary and W. W. Cleland, *Biochemistry*, 1984, **23**, 5479–5488.
29 S. Szapiro and F. Steckel, *Trans. Faraday Soc.*, 1967, **63**, 883–894.
30 E. Gawlita, W. S. Caldwell, M. H. O'Leary, P. Paneth and V. E. Anderson, *Biochemistry*, 1995, **34**, 2577–2583.
31 E. Gawlita, P. Paneth and V. E. Anderson, *Biochemistry*, 1995, **34**, 6050–6058.
32 T. Pineda, R. Callender and S. D. Schwartz, *Biophys. J.*, 2007, **93**, 1474–1483.
33 A. Sievers and R. Wolfenden, *Bioorg. Chem.*, 2005, **33**, 45–52.
34 T. L. Amyes, J. P. Richard and J. J. Tait, *J. Am. Chem. Soc.*, 2005, **127**, 15708–15709.
35 J. A. Smiley, K. M. Hay and B. S. Levison, *Bioorg. Chem.*, 2001, **29**, 96–106.
36 K. N. Houk, J. K. Lee, D. J. Tantillo, S. Bahmanyar and B. N. Hietbrink, *Chem. BioChem.*, 2001, **2**, 113–118.
37 C. L. J. Turnbough, K. H. Kerr, W. R. Funderburg, J. P. Donahue and F. E. Powell, *J. Biol. Chem.*, 1987, **262**, 10239–10245.
38 *Current protocols in molecular biology*, Greene Publishing Associates and Wiley-Interscience, New York, 1994.
39 B. Vemulapalli, M. S. Thesis, Youngstown State University, 2006.
40 R. S. Brody and F. H. Westheimer, *J. Biol. Chem.*, 1979, **254**, 4238–4244.
41 J. B. Bell and M. E. Jones, *J. Biol. Chem.*, 1991, **266**, 12662–12667.
42 T. Ueda, M. Yamamoto, A. Yamane, M. Imazawa and H. Inoue, *J. Carbohydr. Nucleosides, Nucleotides*, 1978, **5**, 261–271.
43 P. S. Anderson, J. M. Smith and B. Mygind, *Eur. J. Biochem.*, 1992, **204**, 51–56.
44 V. L. Smiley, M. S. Thesis, Youngstown State University, 2006.
45 H. K. Jensen, N. Mikkelsen and J. Neuhard, *Protein Expression and Purification*, 1997, **10**, 356–364.
46 M. J. Frisch, G. W. Trucks, H. B. Schlegel, G. E. Scuseria, M. A. Robb, J. R. Cheeseman, J. A. J. Montgomery, T. Vreven, K. N. Kudin, J. C. Burant, J. M. Millam, S. S. Iyengar, J. Tomasi, V. Barone, B. Mennucci, M. Cossi, G. Scalmani, N. Rega, G. A. Petersson, H. Nakatsuji, M. Hada, M. Ehara, K. Toyota, R. Fukuda, J. Hasegawa, M. Ishida, T. Nakajima, Y. Honda, O. Kitao, H. Nakai, M. Klene, X. Li, J. E. Knox, H. P. Hratchian, J. B. Cross, C. Adamo, J. Jaramillo, R. Gomperts, R. E. Stratmann, O. Yazyev, A. J. Austin, R. Cammi, C. Pomelli, J. W. Ochterski, P. Y. Ayala, K. Morokuma, G. A. Voth, P. Salvador, J. J. Dannenberg, V. G. Zakrzewski, S. Dapprich, A. D. Daniels, M. C. Strain, O. Farkas, D. K. Malick, A. D. Rabuck, K. Raghavachari, J. B. Foresman, J. V. Ortiz, Q. Cui, A. G. Baboul, S. Clifford, J. Cioslowski, B. B. Stefanov, G. Liu, A. Liashenko, P. Piskorz, I. Komaromi, R. L. Martin, D. J. Fox, T. Keith, M. A. Al-Laham, C. Y. Peng, A. Nanayakkara, M. Challacombe, P. M. W. Gill, B. Johnson, W. Chen, M. W. Wong, C. Gonzalez, and J. A. Pople, *GAUSSIAN03*, (2004) Gaussian, Inc., Wallingford CT.
47 M. J. Frisch, G. W. Trucks, H. B. Schlegel, G. E. Scuseria, M. A. Robb, J. R. Cheeseman, V. G. Zakrzewski, J. A. J. Montgomery, R. E. Stratmann, J. C. Burant, S. Dapprich, J. M. Millam, A. D. Daniels, K. N. Kudin, M. C. Strain, O. Farkas, J. Tomasi, V. Barone, M. Cossi, R. Cammi, B. Mennucci, C. Pomelli, C. Adamo, S. Clifford, J. Ochterski, G. A. Petersson, P. Y. Ayala, Q. Cui, K. Morokuma, D. K. Malick, A. D. Rabuck, K. Raghavachari, J. B. Foresman, J. Cioslowski, J. V. Ortiz, A. G. Baboul, B. B. Stefanov, G. Liu, A. Liashenko, P. Piskorz, I. Komaromi, R. Gomperts, R. L. Martin, D. J. Fox, T. Keith, M. A. Al-Laham, C. Y. Peng, A. Nanayakkara, C. Gonzalez, M. Challacombe, P. M. W. Gill, B. Johnson, W. Chen, M. W. Wong, J. L. Andres, C. Gonzalez, M. Head-Gordon, E. S. Replogle, and J. A. Pople,*GAUSSIAN98*, (1998) Gaussian, Inc., Pittsburgh, PA.
48 D. A. Singleton, S. A. Merrigan, B. J. Kim, P. Beak, L. M. Phillips and J. K. Lee, *J. Am. Chem. Soc.*, 2000, **122**, 3296–3300.
49 L. M. Phillips and J. K. Lee, *J. Org. Chem.*, 2005, **70**, 1211–1221.
50 R. D. Bach and C. Canepa, *J. Am. Chem. Soc.*, 1997, **119**, 11725–11733.
51 R. D. Bach, C. Canepa and M. N. Glukhovtsev, *J. Am. Chem. Soc.*, 1999, **121**, 6542–6555.
52 L. Onsager, *J. Am. Chem. Soc.*, 1936, **58**, 1486–1493.
53 J. Bigeleisen and M. G. Mayer, *J. Chem. Phys.*, 1947, **15**, 261–267.
54 M. Wolfsberg, *Acc. Chem. Res.*, 1972, **5**, 225–233.
55 M. Saunders, K. E. Laidig and M. Wolfsberg, *J. Am. Chem. Soc.*, 1989, **111**, 8989–8994.
56 D. A. Singleton, Personal Communication.
57 A. P. Scott and L. Radom, *J. Phys. Chem. B*, 1996, **100**, 16502–16513 .
58 E. C. Ralph, J. S. Hirschi, M. A. Anderson, W. W. Cleland, D. A. Singleton and P. F. Fitzpatrick, *Biochemistry*, 2007, **46**, 7655–7664.